State Interaction for Relativistic Four-Component

Methods: Choose the Right Zeroth-Order

Hamiltonian for Late-Row Elements

Chad E. Hoyer, Can Liao, Kirill D. Shumilov, Tianyuan Zhang, and Xiaosong Li*

Department of Chemistry, University of Washington, Seattle, WA, 98195

E-mail: xsli@uw.edu

Abstract

We present several schemes based on the spin-separation of the Dirac-Coulomb-

Breit Hamiltonian for the perturbative treatment of relativistic four-component Hamil-

tonians within the state interaction framework. While state interaction approaches tra-

ditionally use zeroth-order scalar-relativistic states, we develop augmented zeroth-order

Hamiltonians with increasing accuracy and investigate convergence to the variational

limit as a function of the choice of zeroth-order Hamiltonian. The state interaction

schemes developed in this work are benchmarked using ground-state fine-structure

splitting of late-row atoms and diatomic hyrides. Although the scalar-relativistic

zeroth-order Hamiltonian exhibits significant errors in ground-state fine-structure split-

ting, the predictive accuracy can be improved by augmenting the zeroth-order Hamil-

tonian with one- and two-electron vector-relativistic operators (e.g., spin-orbit, spin-

spin, orbit-orbit). This work lays the theoretical foundation for the development of

low-scaling, high-accuracy perturbative relativistic methods suitable for late-row ele-

ments.

1

1 Introduction

Relativistic effects are ubiquitous in electronic structure calculations of late-row-containing molecules, x-ray spectroscopy, and photochemistry. 1-3 How to optimally include relativistic effects in calculations is still an area of ongoing research. One can choose to include relativistic effects variationally (full wave function relaxation) or perturbatively (use a set of zeroth-order wave functions as a basis). In general the perturbative approach will be more practical in terms of computational cost; however, one needs to know when the relativistic effect becomes large enough to deteriorate the perturbative approximation.

The most common relativistic effect included in quantum chemistry is scalar relativity. Scalar relativity is routinely treated variationally. While this choice is often taken for granted due to the ease of implementation, earlier benchmarking elucidated the effect of variational vs perturbative scalar relativity for bond lengths, correlation energies, excitation energies, and electron affinities. The next most common relativistic effect is spin—orbit coupling. Since variational spin—orbit coupling implementations require complex arithmetic and two- or four-component framework (which can both increase the computational cost), 7-33 perturbative approaches for spin—orbit coupling have proven to be more computationally efficient. 34-53

The perturbative relativistic approach has been widely used within the framework of state interaction, often applied with multiconfigurational wave functions, such as the complete active space self-consistent-field wave function with spin-orbit perturbation (CASSCF-SO or SO-MCQDPT). 35,39,53-57 State interaction traditionally represents a spin-orbit operator as perturbation in a basis of scalar-relativistic wave functions (sometimes referred to as a set "spin-free states"). In the full-configuration-interaction limit, state interaction converges to the variational result since the orbital rotations missing in the state interaction become redundant (assuming all possible states are included in the interaction space). As the strength of relativistic effects increases in late-row elements, nonrelativistic or even scalar relativistic wave functions may not be an ideal zeroth-order reference in the state interaction framework.

The two popular partitioning schemes for relativistic operators used in perturbation the-

ory are the Breit–Pauli perturbation expansion and the spin-separation approach. While the Breit–Pauli operator is based on a truncated perturbation expansion of the Dirac Hamiltonian, the spin-separation technique ^{58,59} relies on the use of the Dirac identity to achieve the exact partitioning of the scalar and spin-dependent terms. The Breit–Pauli operator cannot be used to prepare the zeroth-order reference because it is not bounded from below in the variational framework. ⁶⁰ In contrast, scalar and spin-dependent terms arising from the spin-separation approach can be applied in both perturbative and variational electronic structure contexts, leading to a flexible partitioning technique for relativistic Hamiltonians. In particular, with the recent advent of spin-separation of the Dirac–Coulomb–Breit Hamiltonian, ⁵⁹ a hierarchy of perturbative four-component methods for molecular calculations can be effectively developed within the state interaction framework. In this work, we introduce a series of state interaction schemes, emphasizing the quality of various zeroth-order Hamiltonians for late-row elements.

2 Method

2.1 Spin-Separation in the Four-Component Dirac-Coulomb-Breit Hamiltonian

The matrix representation of the kinetically-balanced modified Dirac equation (in a.u.) is:^{21,61}

$$\begin{pmatrix} \mathbf{V} & \mathbf{T} \\ \mathbf{T} & \frac{1}{4c^2}\mathbf{W} - \mathbf{T} \end{pmatrix} \begin{pmatrix} \mathbf{C}_{\mathrm{L}}^+ & \mathbf{C}_{\mathrm{L}}^- \\ \mathbf{C}_{\mathrm{S}}^+ & \mathbf{C}_{\mathrm{S}}^- \end{pmatrix} = \begin{pmatrix} \mathbf{S} & \mathbf{0}_2 \\ \mathbf{0}_2 & \frac{1}{2c^2}\mathbf{T} \end{pmatrix} \begin{pmatrix} \mathbf{C}_{\mathrm{L}}^+ & \mathbf{C}_{\mathrm{L}}^- \\ \mathbf{C}_{\mathrm{S}}^+ & \mathbf{C}_{\mathrm{S}}^- \end{pmatrix} \begin{pmatrix} \boldsymbol{\epsilon}^+ & \mathbf{0} \\ \mathbf{0} & \boldsymbol{\epsilon}^- \end{pmatrix} \tag{1}$$

where c is the speed of light. \mathbf{V} , \mathbf{T} , and \mathbf{S} are the two-component nonrelativistic potential energy, kinetic energy, and overlap matrices, respectively. $\{\epsilon^+\}$, $\{\epsilon^-\}$ are the sets of positive/negative eigenvalues with corresponding molecular orbital coefficients $(\mathbf{C}_{\mathrm{L}}^+ \ \mathbf{C}_{\mathrm{S}}^+)^T$ for

the positive and $(\mathbf{C}_{\mathrm{L}}^{-} \ \mathbf{C}_{\mathrm{S}}^{-})^{T}$ for the negative energy solutions, where L and S denote the large and small component, respectively.

W is the relativistic potential matrix, with elements defined as $\langle \mu | (\boldsymbol{\sigma} \cdot \mathbf{p}) \hat{V}(\boldsymbol{\sigma} \cdot \mathbf{p}) | \nu \rangle$, where **p** is the linear momentum operator, $\boldsymbol{\sigma}$ contains Pauli spin matrices, and $\{\mu, \nu\}$ are atomic orbital bases. For the molecular Hamiltonian, the two potential energy terms are the nuclear–electron and the electron–electron interactions. Using the Dirac relation, a spin separation procedure can be carried out for **W**, ^{58,59}

$$(\boldsymbol{\sigma} \cdot \mathbf{p}) \, \hat{V}(\boldsymbol{\sigma} \cdot \mathbf{p}) = \mathbf{p} \, \hat{V}_{\text{Ne}} \cdot \mathbf{p} + \mathbf{p} \, \hat{V}_{\text{ee}} \cdot \mathbf{p} + i\boldsymbol{\sigma} \cdot \mathbf{p} \, \hat{V}_{\text{Ne}} \times \mathbf{p} + i\boldsymbol{\sigma} \cdot \mathbf{p} \, \hat{V}_{\text{ee}} \times \mathbf{p}$$
(2)

where \hat{V}_{Ne} is the nuclear–electron operator and \hat{V}_{ee} is the electron–electron operator. The first and second dot-product terms are the one- and two-electron scalar-relativities. The third and fourth cross-product terms are the one- and two-electron vector relativities.

Equation (2) presents a framework where relativistic effects can be separated into scalar and vector terms for perturbation theory. Since the scalar-relativistic effects do not break the spin symmetry, they have been used in non-relativistic frameworks with real-value arithmetic to prepare zeroth-order states followed by including spin-orbit, arising from the last two terms in Equation (2), in the perturbative treatment. ^{58,59,62–66} While the spin-separation for one-electron operator is well understood, ⁵⁸ the mathematical procedure to separate scalar and vector relativistic effects for two-electron operators is much more complex.

The frequency-independent Dirac–Coulomb–Breit (DCB) operator in the Coulomb gauge gives rise to the most accurate description of electron–electron interaction before going into

a genuine quantum field treatment. $^{2,33,67-77}$ The DCB operator can be written as

$$\hat{V}_{ee}^{\text{DCB}} = \sum_{i=1}^{N} \sum_{j>i} (\hat{g}^{\text{C}}(i,j) + \hat{g}^{\text{B}}(i,j))$$
(3)

$$\hat{g}^{\mathcal{C}}(i,j) = \frac{1}{r_{ij}} \tag{4}$$

$$\hat{g}^{B}(i,j) = -\frac{1}{2} \left(\frac{\boldsymbol{\alpha}_{i} \cdot \boldsymbol{\alpha}_{j}}{r_{ij}} + \frac{(\boldsymbol{\alpha}_{i} \cdot \mathbf{r}_{ij})(\boldsymbol{\alpha}_{j} \cdot \mathbf{r}_{ij})}{r_{ij}^{3}} \right)$$
 (5)

where $\{i,j\}$ are electron indices. The components of the α matrices are defined as

$$\boldsymbol{\alpha}_{i} = \begin{pmatrix} 0_{2} & \boldsymbol{\sigma}_{i} \\ \boldsymbol{\sigma}_{i} & 0_{2} \end{pmatrix}, \quad i = \{x, y, z\}$$

$$(6)$$

where

$$\sigma_x = \begin{pmatrix} 0 & 1 \\ 1 & 0 \end{pmatrix}, \sigma_y = \begin{pmatrix} 0 & -i \\ i & 0 \end{pmatrix}, \sigma_z = \begin{pmatrix} 1 & 0 \\ 0 & -1 \end{pmatrix}.$$
 (7)

The spin-separation of the Coulomb operator (Equation (4)) results in two-electron scalar relativity, vector spin-own-orbit interaction, and several more complex terms derived from the (SS|SS) integrals. ^{58,59,76,77} Recently, the spin-separation of the Breit operator (Equation (5)) has been developed, revealing that the Breit operator gives rise to spin-other-orbit, spin-spin, and orbit-orbit interactions in both scalar and vector forms. ⁵⁹ For detailed derivations and the complete set of equations, we refer readers to Refs. 76 and 77. Here, we present only the final working expressions in the Supporting Information for the *scalar-relativistic* Dirac-Coulomb-Breit Hamiltonian. The vector-relativistic expressions can be easily derived by removing the terms listed in the Supporting Information from the full set of equations provided in Refs. 76 and 77.

2.2 Perturbation Partitioning Schemes in Four-Component Dirac-Coulomb-Breit Hamiltonian

Typical state interaction approaches for spin—orbit coupling use a non-relativistic or scalar-relativistic Hamiltonian for the zeroth-order Hamiltonian, and the perturbation is a spin—orbit operator (often with approximate two-electron spin—orbit coupling). Although the terms 'scalar relativistic' and 'spin-free relativistic' have often been used interchangeably, we advocate for the consistent use of 'scalar relativistic' because it includes scalar products of spin-dependent terms when two-electron relativistic operator is considered. ⁵⁹ Additionally, we advocate for the use of 'vector relativistic' instead of 'spin—orbit' effect in the perturbation treatment, as the former is more inclusive, encompassing spin—spin and orbit—orbit interactions in the DCB framework.

The perturbation partitioning of the DCB Hamiltonian can be written as,

$$\hat{H}_{DC(B)} = \hat{H}_0 + \hat{V} \tag{8}$$

where \hat{H}_0 is the zeroth-order Hamiltonian and $\hat{V} = \hat{H}_{DC(B)} - \hat{H}_0$ collects the rest of one- and two-electron contributions in the perturbative state-interaction treatment.

In the perturbative state interaction approach, the zeroth-order Hamiltonian \hat{H}_0 is used to obtain the zeroth-order multiconfigurational states, denoted as $|I\rangle$. A one-shot perturbative treatment is employed to couple the zeroth-order states with the perturbation, \hat{V} . The general forms of the state interaction Hamiltonian elements are

$$\left\langle I \left| \hat{H}_0 + \hat{V} \right| I \right\rangle = \sum_{pq} D_{pq}^{II} h_{pq} + \frac{1}{2} \sum_{pqrs} d_{pqrs}^{II} g_{pqrs} \tag{9}$$

$$\left\langle I \left| \hat{V} \right| J \right\rangle = \sum_{pq} D_{pq}^{IJ} \left(h_{pq} - h_{pq}^{0} \right) + \frac{1}{2} \sum_{pqrs} d_{pqrs}^{IJ} \left(g_{pqrs} - g_{pqrs}^{0} \right)$$
 (10)

where I, J are zeroth-order wave functions; p, q, r, s are general molecular orbital indices; D, d are the one- and two-electron transition-density matrices, respectively, that correspond to the zeroth-order wave functions; h, g are the one- and two-electron integrals, respectively; and a superscript of 0 indicates integrals corresponding to \hat{H}_0 .

3 Results and Discussion

In this work, we use minimal-active-space complete-active-space self-consistent field wave functions, which is the standard starting point for a state interaction calculation. We focus on ground-state fine-structure splitting of f-, d-, and p-occupied frontier orbital manifolds of late-row atoms, and p-block diatomic hydrides.

All calculation were performed in a development version of the Chronus Quantum soft-ware package with finite nuclei and a speed of light of 137.035999074 a.u. ⁷⁸ We use a large basis set throughout this work (uncontracted ANO-RCC basis set). ^{79,80} All variational four-component calculations include negative–positive rotations, denoted as CASSCF[±]. ³³ In the Supporting Information, we demonstrate that negative–positive rotations have minimal impact on fine-structure splitting in the systems studied in this work. This insight is crucial when comparing variational and perturbative calculations, as the perturbative Hamiltonian used here does not include an explicit negative–positive rotation term.

In atomic systems, we use active spaces with n-1 electrons in n orbitals, where n is number of orbitals in the valence manifold (e.g., f orbitals for Yb³⁺ and Lu⁴⁺). Note that our implementation is Kramers' unrestricted, so there are 14 f orbitals instead of 7 in the active space. State-average over all possible states generated from this active space was carried out in the 4C-CASSCF[±] optimization.

The diatomic benchmarks focus on four diatomic molecules: GeH, SnH, GeF, and SnF. We used a one-electron active space of four e_1 orbitals (Ge or Sn valence p-orbitals) and two a_1 orbitals (σ^*). We state-average over the lowest four states, covering the lowest non-

relativistic term symbol ${}^{2}\Pi$. The maximum interaction space of six states was used.

Table 1. Zeroth-Order Hamiltonian \mathbf{H}_0 studied in this work.

\ /	variational scalar-relativistic (sr) Dirac-Coulomb(-Breit)
$srD^*C(B)$ -	variational scalar-relativistic (sr) Dirac-Coulomb(-Breit) augmented with one-electron vector-relativistic contributions
srD*C*B-	variational scalar-relativistic (sr) Dirac-Coulomb-Breit augmented with one-electron and two-electron Coulomb vector-relativistic contributions

Table 2. Perturbations V studied in this work.

-vrDC(B)	perturbative vector-relativistic (vr) Dirac-Coulomb(-Breit)
-vrC(B)	perturbative vector-relativistic (vr) Coulomb(-Breit)
-vrB	perturbative vector-relativistic (vr) Breit

3.1 Zeroth-Order Hamiltonians

The accuracy of the perturbative method is heavily dependent on the quality of the zeroth-order wave function used in the state interaction treatment of the perturbation. In this section, we explore various choices for zeroth-order Hamiltonians, as listed in Table 1. To align with the original motivation of spin-separation, 58,59 we develop an all scalar-relativistic zeroth-order Dirac-Coulomb-(Breit) Hamiltonian, srDC(B), which incorporates scalar-relativistic terms from both one- and two-electron contributions. Additionally, we propose two new classes of zeroth-order Hamiltonians by augmenting the scalar-relativistic Hamiltonian with vector-relativistic contributions from one-electron and two-electron operators. Note that within the augmentation naming scheme srD*C*(B*) and DC(B) would be the same Hamiltonians. To evaluate the quality of these zeroth-order Hamiltonians, we compare the computed atomic ground-state fine-structure splitting with the variational formalisms they approximate, as shown in Table 3.

The most accurate calculation in Table 3 is the Dirac–Coulomb–Breit CASSCF[±] (DCB–CASSCF[±]) method, which has a mean unsigned error (MUE) of 0.048 eV. Transitioning from

Table 3. Fine-structure splitting (in eV) for variational relativistic formalisms with CASSCF[±] wave functions with corresponding mean unsigned error (MUE) and percent error (shown in parentheses) relative to experiment. See Table 1 for definition of Hamiltonians.

	srD*C	DC	srD*CB	srD*C*B	DCB	Expt. 81
$-$ Pd ⁺ $^{2}D_{5/2} \rightarrow ^{2}D_{3/2}$	0.588(33.4)	0.434(1.0)	0.588(33.4)	0.435(0.9)	0.419(4.6)	0.439
$Cd^{3+} {}^{2}D_{5/2} \rightarrow {}^{2}D_{3/2}$	0.952(32.1)	0.722(0.2)	0.952(32.1)	0.722(0.2)	0.698(3.2)	0.721
$I^{2}P_{3/2} \rightarrow {}^{2}P_{1/2}$	1.015(7.7)	0.963(2.2)	1.012(7.4)	0.960(1.9)	0.951(0.9)	0.943
${ m Xe^{+}}\ ^2{ m P}_{3/2}^{'} ightarrow\ ^2{ m P}_{1/2}^{'}$	1.407(7.7)	1.336(2.3)	1.403(7.4)	1.332(2.0)	1.319(1.0)	1.306
${\rm Tm}\ ^2{\rm F}_{7/2} o {}^2{\rm F}_{5/2}$	2.002(84.1)	1.117(2.7)	2.004(84.3)	1.118(2.8)	1.062(2.4)	1.087
$Yb^{3+} {}^{2}F_{7/2} \rightarrow {}^{2}F_{5/2}$	2.296(81.3)	1.299(2.6)	2.298(81.4)	1.301(2.7)	1.238(2.2)	1.266
$Lu^{4+} {}^{2}F_{7/2} \rightarrow {}^{2}F_{5/2}$	2.615(78.9)	1.501(2.6)	2.617(79.0)	1.503(2.8)	1.433(2.0)	1.462
${\rm Pt^{+}}\ ^2{\rm D}_{5/2} ightarrow ^2{\rm D}_{3/2}$	1.476(41.4)	1.218(16.7)	1.477(41.4)	1.219(16.8)	1.196(14.5)	1.044
$Hg^{3+} {}^{2}D_{5/2} \rightarrow {}^{2}D_{3/2}$	2.283(17.4)	1.908(1.9)	2.284(17.5)	1.910(1.8)	1.875(3.6)	1.945
$Rn^{+} {}^{2}P_{3/2} \rightarrow {}^{2}P_{1/2}$	4.108(7.3)	3.976(3.8)	4.086(6.7)	3.953(3.2)	3.938(2.8)	3.831
MUE	0.470	0.051	0.468	0.049	0.048	

DCB-CASSCF $^{\pm}$ to the less accurate Dirac-Coulomb CASSCF $^{\pm}$ (DC-CASSCF $^{\pm}$) approach increases MUE by 0.003 eV.

The full-scalar zeroth-order Hamiltonians (srDC and srDCB) are excluded from this comparison, since these reference calculations do not account for fine structure. However, when the scalar zeroth-order Hamiltonians are augmented with vector-relativistic effects from one-electron and two-electron operators, fine-structure splitting is partially recovered in the zeroth-order energies. The extent of this recovery varies among the different zeroth-order Hamiltonians. Specifically, when the scalar Hamiltonian is augmented with one-electron vector-relativistic effects (srD*C and srD*CB), the computed zeroth-order fine-structure splitting shows an overestimate of 0.47 eV compared to experimental data. This overestimation arises from the absence of two-electron spin-orbit coupling, which counteracts the one-electron vector-relativistic effect. ¹⁷ Significant improvement in the zeroth-order energies can be achieved by augmenting the scalar Hamiltonian with both one-electron and two-electron Coulomb vector-relativistic effects. The resulting srD*C*B Hamiltonian yields an error of just 0.001 eV when compared to the results of the full DCB Hamiltonian.

Based on percentage errors, atoms and ions within a same block exhibit similar behavior (see the Block-Dependent Analysis section below for more details). The one exception is

in the 5d block, where Pt⁺ shows a significantly larger percent error for DCB-CASSCF[±] (15% compared to 1-5% for all other systems). This discrepancy is likely due to electron correlation effects, as the $5d \rightarrow 6s$ excitation energy is much lower in Pt⁺ than in Hg³⁺.

While adding vector-relativistic effects to the zeroth-order Hamiltonian is expected to improve the quality of the zeroth-order wave function towards the full variational treatment, it also significantly increases the computational cost. In the all-scalar srDC(B) Hamiltonian, spin symmetry is maintained. This allows for the use of real-valued arithmetic and a reduced-dimension framework, keeping the computational cost comparable to that of a non-relativistic calculation. However, when one-electron vector-relativistic effects are incorporated into the zeroth-order Hamiltonian, it requires the use of a complex-valued four-component self-consistent field, despite the trivial cost of computing one-electron spin-orbit integrals. Moreover, augmenting the zeroth-order Hamiltonian with two-electron Coulomb vector-relativistic effects greatly increases the cost of integral evaluation (refer to Ref. 76 for the cost estimate).

This section establishes a benchmark for the quality of the zeroth-order Hamiltonian. The subsequent sections will examine the effectiveness of the perturbative treatment in correcting errors in fine-structure due to missing relativistic effects, utilizing the state interaction framework.

3.2 Perturbative Dirac-Coulomb Hamiltonians

In Table 3, we presented the performance of the variational Dirac–Coulomb CASSCF[±] (DC-CASSCF[±]), which yielded a mean unsigned error (MUE) of 0.051 eV. In this section, we examine the performance of various perturbative schemes of the Dirac–Coulomb operator, as shown in Table 4. We consider two zeroth-order Hamiltonians: srDC and srD*C. The former is the all-scalar Dirac–Coulomb Hamiltonian, while the latter augments srDC with one-electron vector-relativistic effects. The perturbative schemes are denoted as srDC-CASSCF[±]-vrDC and srD*C-CASSCF[±]-vrC, where the prefixes srDC- and srD*C- refer to

the zeroth-order Hamiltonian used in CASSCF[±], and the suffix -vrDC and -vrC indicates the inclusion of the remaining vector-relativistic (vr) Dirac-Coulomb terms via the state interaction. Notably, the perturbations in srDC-CASSCF[±]-vrDC and srD*C-CASSCF[±]-vrC differ: the former includes the missing one- and two-electron vector-relativistic effects, while the latter includes only the two-electron vector-relativistic contributions in the state interaction treatment. The srDC-CASSCF[±]-vrDC formalism closely relates to traditional CASSCF-SO methods used in the literature but avoids errors due to the picture change. ^{35,39,53-55}

Table 4. Atomic fine-structure splitting (in eV) for perturbative Dirac–Coulomb-based relativistic formalisms with $CASSCF^{\pm}$ wave functions with the mean unsigned error (MUE) and percent error (shown in parentheses) relative to experiment. See Tables 1 and 2 for definition of Hamiltonians.

	srDC-CASSCF [±] -vrDC	$srD^*C\text{-}CASSCF^{\pm}\text{-}vrC$	$\mathrm{DC\text{-}CASSCF}^{\pm}$	Expt. 81
$Pd^{+} ^{2}D_{5/2} \rightarrow ^{2}D_{3/2}$	0.447(1.9)	0.431(1.9)	0.434(1.0)	0.439
${\rm Cd}^{3+} {}^{2}{\rm D}_{5/2} \to {}^{2}{\rm D}_{3/2}$	0.725(0.6)	0.715(0.7)	0.722(0.2)	0.721
$I^{2}P_{3/2} \rightarrow {}^{2}P_{1/2}$	0.880(6.6)	0.962(2.0)	0.963(2.2)	0.943
$Xe^{+} {}^{2}P_{3/2} \rightarrow {}^{2}P_{1/2}$	1.224(6.3)	1.335(2.2)	1.336(2.3)	1.306
${\rm Tm}\ ^2{\rm F}_{7/2} o {}^2{\rm F}_{5/2}$	1.097(0.9)	1.041(4.3)	1.117(2.7)	1.087
$Yb^{3+2}F_{7/2} \rightarrow {}^{2}F_{5/2}$	1.281(1.1)	1.212(4.3)	1.299(2.6)	1.266
$Lu^{4+} {}^{2}F_{7/2} \rightarrow {}^{2}F_{5/2}$	1.477(1.0)	1.402(4.1)	1.501(2.6)	1.462
${ m Pt}^{+} { m ^2D}_{5/2} ightarrow { m ^2D}_{3/2}$	1.349(29.3)	1.197(14.6)	1.218(16.7)	1.044
${\rm Hg^{3+~^2D_{5/2}} \rightarrow {^2D_{3/2}}}$	2.038(4.8)	1.884(3.1)	1.908(1.9)	1.945
${\rm Rn}^{+} {}^{2}{\rm P}_{3/2} \rightarrow {}^{2}{\rm P}_{1/2}$	3.424(10.6)	3.968(3.6)	3.976(3.8)	3.831
MUE	0.100	0.057	0.051	

We find that srDC-CASSCF[±]-vrDC has a significantly larger MUE compared to the variational DC-CASSCF[±] (0.100 eV for srDC-CASSCF[±]-vrDC versus 0.051 eV for DC-CASSCF[±]). However, when the all-scalar srDC is augmented with one-electron spin-orbit effects in the zeroth-order Hamiltonian, the error is notably reduced (0.057 eV for srD*C-CASSCF[±]-vrC compared to 0.051 eV for DC-CASSCF[±]). This analysis indicates that a wave function computed without vector-relativistic effects may not serve as a suitable zeroth-order reference for the perturbative state interaction treatment, especially for late-row elements. To accurately recover the missing fine-structure splitting, a larger interaction space might be required if the all-scalar-relativistic zeroth-order Hamiltonian is used (this would require a larger active space for these systems).

3.3 Perturbative Dirac-Coulomb-Breit Hamiltonians

For the Dirac–Coulomb–Breit (DCB) operator, three different zeroth-order Hamiltonians can be constructed: the all-scalar-relativistic DCB (srDCB), srDCB augmented with one-electron vector-relativistic terms (srD*CB), and srDCB augmented with both one-electron and two-electron Coulomb vector-relativistic terms (srD*C*B). We investigate these three different perturbation partitionings and compare them to the variational DCB-CASSCF[±] method and experimental data for ground-state fine-structure splittings, as shown in Table 5.

Table 5. Fine-structure splitting (in eV) for perturbative Dirac–Coulomb–Breit-based relativistic formalisms with CASSCF[±] wave functions with corresponding mean unsigned error (MUE) and percent error (shown in parentheses) relative to experiment. The top row denotes the zeroth-order Hamiltonian and the row below denotes the remaining vector-relativistic terms that are included perturbatively. See Tables 1 and 2 for definition of Hamiltonians.

	srDCB	srD*CB	srD^*C^*B	- DCB-CASSCF [±]	Expt. 81
	vrDCB	vrCB	vrB		
$Pd^{+} ^{2}D_{5/2} \rightarrow ^{2}D_{3/2}$	0.432(1.5)	0.416(5.2)	0.420(4.3)	0.419(4.6)	0.439
$Cd^{3+} {}^{2}D_{5/2} \rightarrow {}^{2}D_{3/2}$	0.703(2.5)	0.693(3.8)	0.700(2.9)	0.698(3.2)	0.721
$I^{2}P_{3/2} \rightarrow {}^{2}P_{1/2}$	0.869(7.8)	0.950(0.7)	0.951(0.9)	0.951(0.9)	0.943
$Xe^{+} {}^{2}P_{3/2} \rightarrow {}^{2}P_{1/2}$	1.209(7.5)	1.319(1.0)	1.320(1.1)	1.319(1.0)	1.306
${\rm Tm}\ ^2{\rm F}_{7/2} \to {}^2{\rm F}_{5/2}$	1.053(3.2)	0.995(8.5)	1.071(1.5)	1.062(2.4)	1.087
$Yb^{3+} {}^{2}F_{7/2} \rightarrow {}^{2}F_{5/2}$	1.230(2.9)	1.161(8.3)	1.250(1.3)	1.238(2.2)	1.266
$Lu^{4+} {}^{2}F_{7/2} \rightarrow {}^{2}F_{5/2}$	1.421(2.8)	1.346(7.9)	1.446(1.1)	1.433(2.0)	1.462
${\rm Pt^{+}}\ ^{2}{\rm D}_{5/2} \rightarrow {}^{2}{\rm D}_{3/2}$	1.323(26.8)	1.174(12.5)	1.196(14.5)	1.196(14.5)	1.044
$Hg^{3+} {}^{2}D_{5/2} \rightarrow {}^{2}D_{3/2}$	1.999(2.8)	1.850(4.9)	1.876(3.6)	1.875(3.6)	1.945
$Rn^{+} {}^{2}P_{3/2} \rightarrow {}^{2}P_{1/2}$	3.385(11.6)	3.930(2.6)	3.938(2.8)	3.938(2.8)	3.831
MUE	0.109	0.071	0.044	0.048	

State interaction calculations using the all-scalar-relativistic zeroth-order srDCB Hamiltonian show a large mean unsigned error (MUE) of 0.109 eV for the benchmark test set. This significant error again suggests that the all scalar-relativistic wave function may not be a suitable zeroth-order reference for the perturbative state interaction treatment. By including the one-electron spin-orbit coupling in the zeroth-order Hamiltonian, the MUE reduces from 0.109 eV to 0.071 eV (srDCB-CASSCF[±]-vrDCB vs. srD*CB-CASSCF[±]-vrCB). The third

partitioning includes the two-electron spin—orbit coupling contribution from the Coulomb operator in the zeroth-order Hamiltonian (srD*C*B-CASSCF±-vrB), resulting in an MUE difference of only 0.004 eV compared to DCB-CASSCF±, indicating near perturbation convergence.

Despite its high computational cost, using the zeroth-order Hamiltonian with two-electron Coulomb vector-relativistic terms (srD*C*B) is advantageous. This approach avoids the computation of the most expensive Breit integrals in the CASSCF[±] procedure while the state interaction with one-shot perturbative Breit treatment can produce fine-structure splittings comparable to full variational calculations. Assuming 20 iterations in the CASSCF[±] step and that all integrals are computed once and stored in memory, *i.e.*, the in-core method, the cost analysis in terms of floating-point operations (FLOP) count from Ref. 77 indicates that the one-shot perturbative Breit method using the state interaction approach is 4 times faster than the full DCB-CASSCF[±]. The computational savings primarily arise from the reduced number of in-core integral transformations for the Breit Hamiltonian. For the AO-direct CASSCF[±] procedure, these savings are even more substantial, as the computation of Breit integrals is 2 orders of magnitude more expensive than those for the Dirac-Coulomb Hamiltonian. As a result, one should expect a 2-3 order magnitude speedup when using the perturbative Breit method within the state interaction framework compared to the fully variational DCB-CASSCF[±].

3.4 Block-Dependent Analysis

In Table 6 we show the MUE of the computed ground-state fine-structure splitting as a function of blocks of the periodic table. For 4d and 5p blocks (fifth-row), perturbative state-interaction approaches perform well, with small errors comparable to variational methods. However, the error increases significantly for the 5d and 6p blocks. For these blocks, state-interaction methods using all-scalar references (srDC- and srDCB-) exhibit large errors in the range of 0.40-0.45 eV, rendering them unreliable for computational studies of

Table 6. Mean-unsigned error (MUE) (in eV) of the computed ground-state fine-structure splitting using perturbative and variational Dirac-Coulomb(-Breit) relativistic formalisms with CASSCF[±] wave functions. The top row denotes the zeroth-order Hamiltonian and the row below denotes the remaining vector-relativistic terms that are included perturbatively. See Tables 1 and 2 for definition of Hamiltonians.

srDC vrDC	srD*C vrC	DC-CASSCF [±]	srDCB vrDCB	srD*CB vrCB	srD*C*B vrB	- DCB-CASSCF [±]
$\begin{array}{c cc} 4d & 0.007 \\ 5p & 0.072 \\ 4f & 0.013 \\ 5d & 0.199 \\ 6p & 0.407 \end{array}$	0.007 0.024 0.054 0.107 0.137	0.003 0.025 0.033 0.105 0.145	0.012 0.086 0.038 0.167 0.446	0.025 0.010 0.105 0.112 0.099	0.020 0.011 0.016 0.110 0.107	0.022 0.011 0.028 0.111 0.107

molecular complexes containing elements in the sixth-row or above. This observation agrees with previous work using all-scalar-relativistic zeroth-order Hamiltonianss. ^{39,40,52,53} In contrast, methods using reference Hamiltonians augmented with one-electron and two-electron Dirac–Coulomb vector relativistic corrections can nearly replicate the results obtained with variational methods.

Overall, for all methods considered here, the error increases with increasing principle quantum number and angular momentum with an exception for the 4f manifold. State-interaction methods using all-scalar references (srDC- and srDCB-) exhibit an exceptionally small error, even out-performing some high-level methods. Adding extra tight or diffuse f functions does not seem to change the behavior as shown in the Supporting Information, suggesting that this is not a basis set issue. Nevertheless, all methods considered here do well for the 4f fine-structure splitting.

3.5 Perturbative Hamiltonians Applied to Diatomic Hydrides

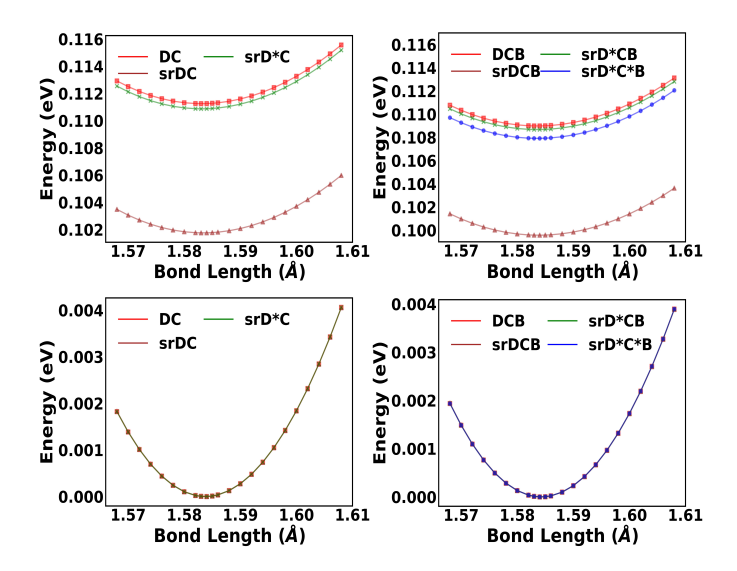


Figure 1. Potential energy surface of GeH. The $E_{1/2}$ ground state surfaces are shown on the bottom plots. The $E_{3/2}$ surfaces are shown on the top plots. Surfaces on the left are calculated using Dirac–Coulomb-based formalisms. Surfaces on the right are calculated using Dirac–Coulomb-Breit-based formalisms.

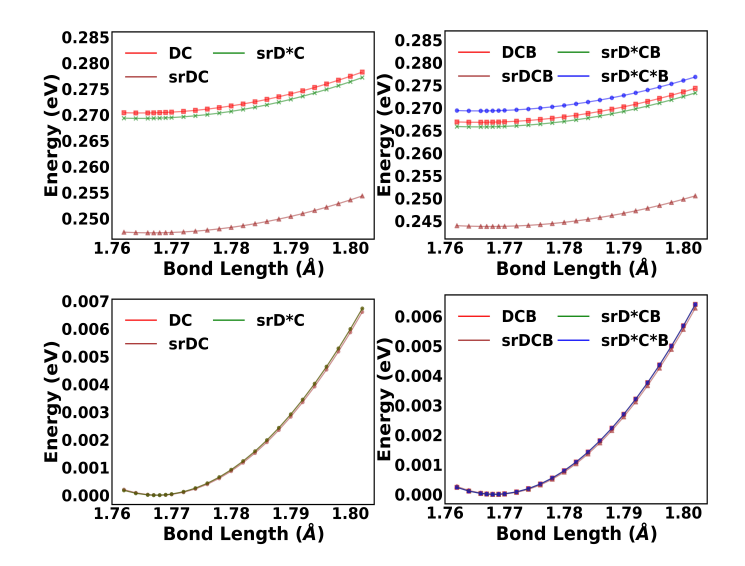


Figure 2. Potential energy surface of SnH. The $E_{1/2}$ ground state surfaces are shown on the bottom plots. The $E_{3/2}$ surfaces are shown on the top plots. Surfaces on the left are calculated using Dirac-Coulomb-based formalisms. Surfaces on the right are calculated using Dirac-Coulomb-Breit-based formalisms.

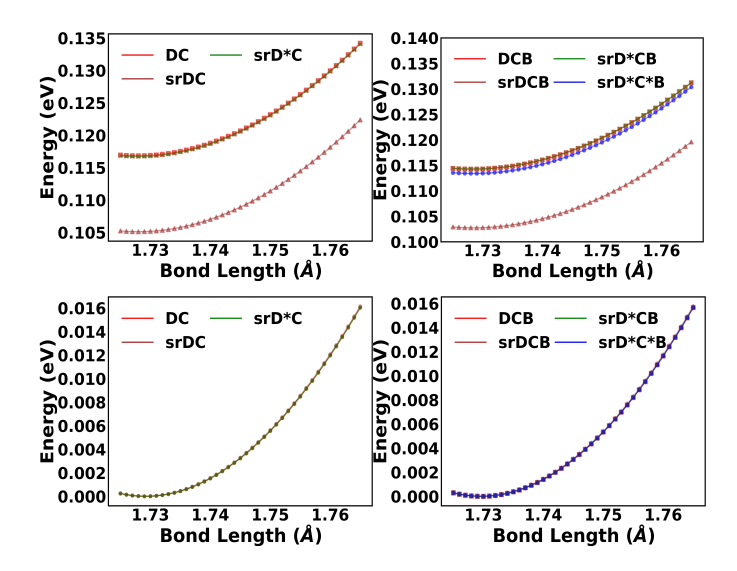


Figure 3. Potential energy surface of GeF. The $E_{1/2}$ ground state surfaces are shown on the bottom plots. The $E_{3/2}$ surfaces are shown on the top plots. Surfaces on the left are calculated using Dirac–Coulomb-based formalisms. Surfaces on the right are calculated using Dirac–Coulomb–Breit-based formalisms.

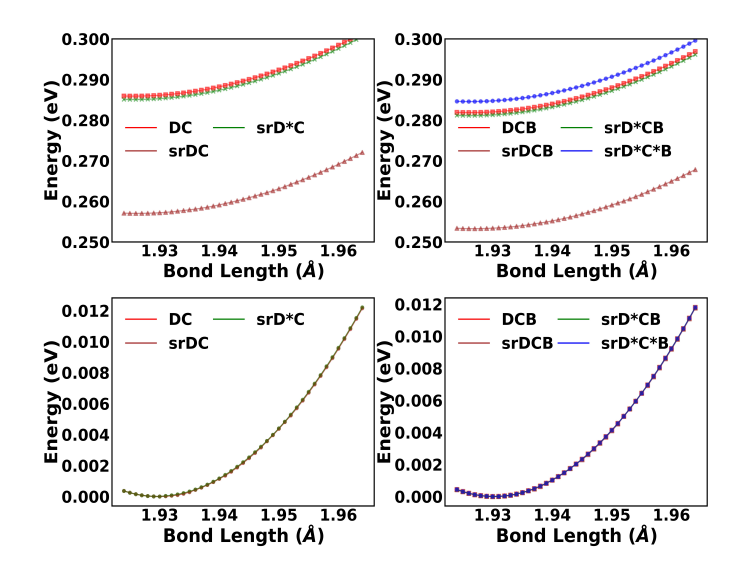


Figure 4. Potential energy surface of SnF. The $E_{1/2}$ ground state surfaces are shown on the bottom plots. The $E_{3/2}$ surfaces are shown on the top plots. Surfaces on the left are calculated using Dirac–Coulomb-based formalisms. Surfaces on the right are calculated using Dirac–Coulomb–Breit-based formalisms.

We expand our benchmark of the Dirac–Coulomb-based formalisms to diatomic molecules GeH, SnH, GeF, and SnF. Without vector-relativity, these molecules exhibit a four-fold degenerate ${}^{2}\Pi$ ground state. Vector-relativity splits the four-fold degeneracy into two Kramers pairs denoted by the double group irreducible representation $E_{1/2}$ for the ground state and

 $E_{3/2}$ for the excited state.

To visualize the splitting as bond length varies, we report potential-energy curves in Figures 1 to 4. Using the presented formalisms, equilibrium bond lengths were computed along with the ${}^2\Pi$ splitting at equilibrium. The equilibrium bond length was not affected by the choice of formalism, with only the srDC-CASSCF $^\pm$ -vrDC SnH bond length differing from the two other formalisms by 0.001 Å.

Table 7 presents the computed fine-structure splitting of the ${}^2\Pi$ ground state using the Dirac-Coulomb-based methods. Consistent with the atomic results, srDC-CASSCF $^\pm$ -vrDC underperformed compared to the other two formalisms in predicting the ${}^2\Pi$ splitting, underestimating it by 0.009, 0.023, 0.011, and 0.035 eV for GeH, SnH, GeF, and SnF, respectively. Augmenting with one-electron vector relativity reduces the error to the meV range, aligning closely with the results from full variational DC-CASSCF $^\pm$. Interestingly, the average error of srDC-CASSCF $^\pm$ -vrDC in predicting p-block molecular splittings is noticeably smaller than that observed for atomic species in Table 6.

Table 7. GeH and SnH ground state fine-structure splitting (in eV) and equilibrium bond lengths (in Å) calculated using perturbative Dirac–Coulomb-based relativistic formalisms with CASSCF $^{\pm}$ wave functions. See Tables 1 and 2 for definition of Hamiltonians.

	srDC-CASSCF [±] -vrDC	$srD^*C\text{-}CASSCF^{\pm}\text{-}vrC$	$\mathrm{DC\text{-}CASSCF}^{\pm}$	Expt. 81
GeH ² ∏ Splitting Bond Length	0.102 1.584	0.111 1.584	0.111 1.584	0.111 1.588
SnH ² ∏ Splitting Bond Length	0.247 1.768	0.269 1.767	0.270 1.767	0.270 1.782
GeF ² Π Splitting Bond Length	0.105 1.729	0.117 1.729	0.117 1.729	0.116 1.745
SnF ² II Splitting Bond Length	0.252 1.930	0.285 1.930	0.286 1.930	0.287 1.944

Similar to the results in Table 7, in Table 8 the different Dirac-Coulomb-Breit formalisms minimally affect equilibrium bond length, with the SnH bond length differing by

0.001 Å when using an all-scalar-relativistic zeroth-order DCB Hamiltonian compared to the other formalisms. The all-scalar-relativistic zeroth-order formalism continues to underestimate the ${}^{2}\Pi$ splitting compared to the other formalisms but noticeably less than the srDCB-CASSCF $^{\pm}$ -vrDCB 5p atomic benchmark in Table 6.

Table 8. GeH and SnH ground state fine-structure splitting (in eV) and equilibrium bond lengths (in Å) calculated using perturbative Dirac-Coulomb-Breit-based relativistic formalisms with CASSCF[±] wave functions. The top row denotes the zeroth-order Hamiltonian and the row below denotes the remaining vector-relativistic terms that are included perturbatively. See Tables 1 and 2 for definition of Hamiltonians.

	srDCB vrDCB	srD*CB vrCB	srD*C*B vrB	- DCB-CASSCF [±]	Expt. 81
$ m GeH~^2\Pi$					
Splitting	0.100	0.109	0.109	0.109	0.111
Bond Length	1.584	1.584	1.584	1.584	1.588
$\mathbf{SnH}^{\ 2}\Pi$					
Splitting	0.244	0.266	0.267	0.267	0.270
Bond Length	1.769	1.768	1.768	1.768	1.782
$ m GeF~^2\Pi$					
Splitting	0.103	0.114	0.114	0.114	0.116
Bond Length	1.730	1.730	1.730	1.730	1.745
$\mathbf{SnF}^{\ 2}\Pi$					
Splitting	0.249	0.281	0.282	0.282	0.287
Bond Length	1.930	1.930	1.930	1.930	1.944

4 Conclusion

In this work, based on the recent development of spin-separation of the Dirac-Coulomb-Breit operator, we introduced several zeroth-order four-component Hamiltonians suitable for state-interaction perturbation theory using CASSCF wave functions: scalar-relativistic Dirac-Coulomb (srDC), scalar-relativistic Dirac-Coulomb-Breit (srDCB), srDC augmented with one-electron vector-relativity (srD*C), srDCB augmented with one-electron vector-relativity (srD*CB), and srDCB augmented with one- and two-electron Coulomb vector-

relativity (srD^*C^*B) .

Benchmark calculations using atomic and diatomic fine-structure splitting show that the accuracy of the proposed state-interaction schemes increases converging toward the variational full DCB-CASSCF $^{\pm}$ results. For late-row elements, the all scalar-relativistic zeroth-order Hamiltonian used in the state interaction CASSCF $^{\pm}$ method exhibits a large error in fine-structure splitting. The accuracy can be improved by augmenting the all scalar-relativistic zeroth-order Hamiltonian with one- and two-electron Coulomb vector-relativities.

Orbital-dependent analysis supports the use of all-scalar relativistic zeroth-order Hamiltonians for 4d, 5p, and core-like 4f manifolds. However, for heavier elements in the sixth-row and above, we recommend using vector-relativity-augmented zeroth-order Hamiltonians.

Despite its high computational cost, using the zeroth-order Hamiltonian augmented with one-electron and two-electron Coulomb vector-relativistic terms (srD*C*B) is advantageous. This approach avoids the computation of the most expensive Breit integrals in the CASSCF[±] procedure, while the state interaction with one-shot perturbative Breit treatment can produce fine-structure splittings comparable to full variational calculations.

It is important to note that these findings are based on small state-interaction spaces, consistent with a low-scaling relativistic approach suitable for perturbation theory. Convergence as a function of state-interaction space remains to be demonstrated in future work.

Acknowledgement

This work is supported by the U.S. Department of Energy, Office of Science, Basic Energy Sciences, in the Computational and Theoretical program (Grant No. DE-SC0006863) for the development of the Breit operator for Dirac and quantum field theory. The development of the Chronus Quantum computational software is supported by the Office of Advanced Cyber-infrastructure, National Science Foundation (Grant No. OAC-2103717). Computations were facilitated through the use of advanced computational, storage, and networking infrastructure.

ture provided by the shared facility supported by the University of Washington Molecular Engineering Materials Center (DMR-2308979) via the Hyak supercomputer system.

Supporting Information Available

Supporting information includes the effect of negative–positive-orbital rotations, basis-set tests for $\mathrm{Lu^{4+}}$, and expressions for the scalar-relativistic Dirac–Coulomb–Breit Hamiltonian in the Pauli quaternion representation.

References

- (1) Yarkony, D. R. Spin-Forbidden Chemistry within the Breit-Pauli Approximation. *Int. Rev. Phys. Chem.* **1992**, *11*, 195–242.
- (2) Pyykkö, P. Relativistic Effects in Chemistry: More Common Than You Thought. *Annu. Rev. Phys. Chem.* **2012**, *63*, 45–64.
- (3) Marian, C. M. Spin-Orbit Coupling and Intersystem Crossing in Molecules. WIREs Comp. Mol. Sci. 2012, 2, 187–203.
- (4) Snijders, J.; Pyykkö, P. Is the Relativistic Contraction of Bond Lengths an Orbital-Contraction Effect? *Chem. Phys. Lett.* **1980**, *75*, 5–8.
- (5) Blomberg, M. R.; Wahlgren, U. On the Effect of Core Orbital Relaxation in First-Order Relativistic Calculations. Chem. Phys. Lett. 1988, 145, 393–398.
- (6) Marian, C. M. On the Dependence of Correlation and Relativity: The Electron Affinity of the Copper Atom. *Chem. Phys. Lett.* **1990**, *173*, 175–180.
- (7) Mohanty, A.; Clementi, E. Dirac-Fock Self-Consistent Field Method for Closed-Shell Molecules with Kinetic Balance and Finite Nuclear Size. Int. J. Quant. Chem. 1991, 39, 487–517.
- (8) Eliav, E.; Kaldor, U. The Relativistic Four-Component Coupled Cluster Method for Molecules: Spectroscopic Constants of SnH4. *Chem. Phys. Lett.* **1996**, *248*, 405–408.
- (9) Visscher, L.; Lee, T. J.; Dyall, K. G. Formulation and Implementation of a Relativistic Unrestricted Coupled-Cluster Method including Noniterative Connected Triples. J. Chem. Phys. 1996, 105, 8769.
- (10) Jensen, H. J. A.; Dyall, K. G.; Saue, T.; Fægri, K. Relativistic Four-component Multiconfigurational Self-Consistent-Field Theory for Molecules: Formalism. J. Chem. Phys. 1996, 104, 4083–4097.

- (11) Saue, T.; Fægri, K.; Helgaker, T.; Gropen, O. Principles of Direct 4-Component Relativistic SCF: Application to Caesium Auride. *Mol. Phys.* **1997**, *91*, 937–950.
- (12) Saue, T.; Jensen, H. J. A. Quaternion Symmetry in Relativistic Molecular Calculations: The Dirac–Hartree–Fock Method. *J. Chem. Phys.* **1999**, *111*, 6211–6222.
- (13) Fleig, T.; Olsen, J.; Visscher, L. The Generalized Active Space Concept for the Relativistic Treatment of Electron Correlation. II. Large-Scale Configuration Interaction Implementation Based on Relativistic 2- and 4-Spinors and its Application. J. Chem. Phys. 2003, 119, 2963–2971.
- (14) Gao, J.; Wenjian, L.; Song, B.; Liu, C. Time-Dependent Four-Component Relativistic Density Functional Theory for Excitation Energies. *J. Chem. Phys.* **2004**, *121*, 6658–6666.
- (15) Gao, J.; Zou, W.; Liu, W.; Xiao, Y.; Peng, D.; Song, B.; Liu, C. Time-Dependent Four-Component Relativistic Density-Functional Theory for Excitation Energies. II. The Exchange-Correlation Kernel. J. Chem. Phys. 2005, 123, 054102.
- (16) Fleig, T.; Jensen, H. J. A.; Olsen, J.; Visscher, L. The Generalized Active Space Concept for the Relativistic Treatment of Electron Correlation. III. Large-Scale Configuration Interaction and Multiconfiguration Self-Consistent-Field Four-Component Methods with Application to UO2. J. Chem. Phys. 2006, 124, 104106.
- (17) Dyall, K. G.; Fægri Jr, K. Introduction to Relativistic Quantum Chemistry; Oxford University Press, 2007.
- (18) Thyssen, J.; Fleig, T.; Jensen, H. J. A. A Direct Relativistic Four-component Multiconfiguration Self-Consistent-Field Method for Molecules. J. Chem. Phys. 2008, 129, 034109.

- (19) Sørensen, L. K.; Knecht, S.; Fleig, T.; Marian, C. M. Four-Component Relativistic Coupled Cluster and Configuration Interaction Calculations on the Ground and Excited States of the RbYb Molecule. J. Phys. Chem. A 2009, 113, 12607–12614.
- (20) Saue, T. Relativistic Hamiltonians for Chemistry: A Primer. *ChemPhysChem* **2011**, 12, 3077–3094.
- (21) Reiher, M.; Wolf, A. *Relativistic Quantum Chemistry*, 2nd ed.; Wiley-VCH: Weinheim, 2015.
- (22) Bates, J. E.; Shiozaki, T. Fully Relativistic Complete Active Space Self-Consistent Field for Large Molecules: Quasi-Second-Order Minimax Optimization. J. Chem. Phys. 2015, 142, 044112.
- (23) Zhang, B.; Vandezande, J. E.; Reynolds, R. D.; Schaefer, H. F. Spin-Orbit Coupling via Four-Component Multireference Methods: Benchmarking on p-Block Elements and Tentative Recommendations. J. Chem. Theory Comput. 2018, 14, 1235–1246.
- (24) Egidi, F.; Sun, S.; Goings, J. J.; Scalmani, G.; Frisch, M. J.; Li, X. Two-Component Non-Collinear Time-Dependent Spin Density Functional Theory for Excited State Calculations. *J. Chem. Theory Comput.* **2017**, *13*, 2591–2603.
- (25) Hu, H.; Jenkins, A. J.; Liu, H.; Kasper, J. M.; Frisch, M. J.; Li, X. Relativistic Two-Component Multireference Configuration Interaction Method with Tunable Correlation Space. J. Chem. Theory Comput. 2020, 16, 2975–2984.
- (26) Liu, J.; Cheng, L. Relativistic Coupled-Cluster and Equation-of-Motion Coupled-Cluster Methods. WIREs Comput. Mol. Sci. 2021, 11, 1536.
- (27) Hoyer, C. E.; Li, X. Relativistic Two-Component Projection-Based Quantum Embedding for Open-Shell Systems. *J. Chem. Phys.* **2020**, *153*, 094113.

- (28) Grofe, A.; Gao, J.; Li, X. Exact-Two-Component Block-Localized Wave Function: A Simple Scheme for the Automatic Computation of Relativistic ΔSCF. J. Chem. Phys. 2021, 155, 014103.
- (29) Sharma, P.; Jenkins, A. J.; Scalmani, G.; Frisch, M. J.; Truhlar, D. G.; Gagliardi, L.; Li, X. Exact-Two-Component Multiconfiguration Pair-Density Functional Theory. J. Chem. Theory Comput. 2022, 18, 2947–2954.
- (30) Grofe, A.; Li, X. Relativistic Nonorthogonal Configuration Interaction: Application to L_{2,3}-edge X-ray Spectroscopy. *Phys. Chem. Chem. Phys.* **2022**, *24*, 10745–10756.
- (31) Lu, L.; Hu, H.; Jenkins, A. J.; Li, X. Exact-Two-Component Relativistic Multireference Second-Order Perturbation Theory. J. Chem. Theory Comput. 2022, 18, 2983–2992.
- (32) Hoyer, C. E.; Hu, H.; Lu, L.; Knecht, S.; Li, X. Relativistic Kramers-Unrestricted Exact-Two-Component Density Matrix Renormalization Group. *J. Phys. Chem. A* **2022**, *126*, 5011–5020.
- (33) Hoyer, C. E.; Lu, L.; Hu, H.; Shumilov, K. D.; Sun, S.; Knecht, S.; Li, X. Correlated Dirac-Coulomb-Breit Multiconfigurational Self-Consistent-Field Methods. *J. Chem. Phys.* **2023**, *158*, 044101.
- (34) Heß, B. A.; Marian, C. M.; Wahlgren, U.; Gropen, O. A Mean-Field Spin-Orbit Method Applicable to Correlated Wavefunctions. *J. Chem. Phys.* **1996**, *251*, 365–371.
- (35) Berning, A.; Schweizer, M.; Werner, H.-J.; Knowles, P. J.; Palmieri, P. Spin-Orbit Matrix Elements for Internally Contracted Multireference Configuration Interaction Wavefunctions. Mol. Phys. 2000, 98, 1823–1833.
- (36) Koseki, S.; Federov, D. G.; Schmidt, M. W.; Gordon, M. S. Spin-Orbit Splittings in the Third-Row Transition Elements: Comparison of Effective Nuclear Charge and Full Breit-Pauli Calculations. J. Phys. Chem. A 2001, 105, 8262–8268.

- (37) Malmqvist, P. Å.; Roos, B. O.; Schimmelpfennig, B. The Restricted Active Space (RAS) State Interaction Approach with Spin-orbit Coupling. *Chem. Phys. Lett.* **2002**, *357*, 230–240.
- (38) Gagliardi, L.; Roos, B. O. The Electronic Spectrum of $Re_2Cl_8^{2-}$: A Theoretical Study. Inorg. Chem. **2003**, 42, 1599–1603.
- (39) Roos, B. O.; Malmqvist, P.-Å. Relativistic Quantum Chemistry: The Multiconfigurational Approach. *Phys. Chem. Chem. Phys.* **2004**, *6*, 2919–2927.
- (40) Wang, F.; Ziegler, T. A Simplified Relativistic Time-Dependent Density-Functional Theory Formalism for the Calculations of Excitation Energies Including Spin-Orbit Coupling Effect. J. Chem. Phys. 2005, 123, 154102.
- (41) Klein, K.; Gauss, J. Perturbative Calculation of Spin-Orbit Splittings using the Equation-of-Motion Ionization-Potential Coupled-Cluster Ansatz. J. Chem. Phys. 2008, 129, 194106.
- (42) Wang, F.; Gauss, J.; van Wüllen, C. Closed-shell Coupled-cluster Theory with Spin-orbit Coupling. J. Chem. Phys. 2008, 129, 064113.
- (43) Wang, Z.; Wang, F. Spin-orbit Coupling and Electron Correlation at Various Coupledcluster Levels for Closed-shell Diatomic Molecules. *Phys. Chem. Chem. Phys.* 2013, 15, 17922–17928.
- (44) Cheng, L.; Gauss, J. Perturbative Treatment of Spin-Orbit Coupling within Spin-Free Exact Two-Component Theory. J. Chem. Phys. 2014, 141, 164107.
- (45) Epifanovsky, E.; Klein, K.; Stopkowicz, S.; Gauss, J.; Krylov, A. Spin-Orbit Couplings within the Equation-of-Motion Coupled-Cluster Framework: Theory, Implementation, and Benchmark Calculations. *J. Chem. Phys.* **2015**, *143*, 064102.

- (46) Cheng, L.; Wang, F.; Stanton, J. F.; Gauss, J. Perturbative Treatment of Spin-orbit-coupling within Spin-free Exact Two-component Theory using Equation-of-motion Coupled-cluster Methods. J. Chem. Phys. 2018, 148, 044108.
- (47) Mussard, B.; Sharma, S. One-Step Treatment of Spin-Orbit Coupling and Electron Correlation in Large Active Spaces. *J. Chem. Theory Comput.* **2018**, *14*, 154–165.
- (48) Bokhan, D.; Trubnikov, D. N.; Perera, A.; Bartlett, R. J. Spin-orbit Split Ionized and Electron-attached States using Explicitly-Correlated Equation-of-motion Coupledcluster Singles and Doubles Eigenvectors. Chem. Phys. Lett. 2019, 730, 372–377.
- (49) Vidal, M. L.; Pokhilko, P.; Krylov, A. I.; Coriani, S. Equation-of-Motion Coupled-Cluster Theory to Model L-Edge X-ray Absorption and Photoelectron Spectra. J. Phys. Chem. Lett. 2020, 11, 8314–8321.
- (50) Meitei, O. R.; Houck, S. E.; Mayhall, N. J. Spin-Orbit Matrix Elements for a Combined Spin-Flip and IP/EA Approach. *J. Chem. Theory Comput.* **2020**, *16*, 3597–3606.
- (51) Carreras, A.; Jiang, H.; Pokhilko, P.; Krylov, A. I.; Zimmerman, P. M.; Casanova, D. Calculation of Spin-orbit Couplings using RASCI Spinless One-particle Density Matrices: Theory and Applications. J. Chem. Phys. 2020, 153, 214107.
- (52) Liao, C.; Kasper, J. M.; Jenkins, A. J.; Yang, P.; Batista, E. R.; Frisch, M. J.; Li, X. State Interaction Linear Response Time-Dependent Density Functional Theory with Perturbative Spin-Orbit Coupling: Benchmark and Perspectives. JACS Au 2023, 3, 358–367.
- (53) Liao, C.; Hoyer, C. E.; Banerjee Ghosh, R.; Jenkins, A. J.; Knecht, S.; Frisch, M. J.; Li, X. Comparison of Variational and Perturbative Spin-Orbit Coupling within Two-Component CASSCF. J. Phys. Chem. A 2024, 128, 2498-2506.

- (54) Fedorov, D. G.; Finley, J. P. Spin-Orbit Multireference Multistate Perturbation Theory. Phys. Rev. A 2001, 64, 042502.
- (55) Fedorov, D. G.; Koseki, S.; Schmidt, M. W.; Gordon, M. S. Spin-orbit Coupling in Molecules: Chemistry Beyond the Adiabatic Approximation. Int. Rev. Phys. Chem. 2003, 22, 551–592.
- (56) Ganyushin, D.; Neese, F. First-Principles Calculations of Zero-Field Splitting Parameters. J. Chem. Phys. **2006**, 125, 024103.
- (57) Sayfutyarova, E. R.; Chan, G. K.-L. A State Interaction Spin-Orbit Coupling Density Matrix Renormalization Group Method. J. Chem. Phys. 2016, 144, 234301.
- (58) Dyall, K. G. An Exact Separation of the Spin-free and Spin-dependent Terms of the Dirac-Coulomb-Breit Hamiltonian. J. Chem. Phys. 1994, 100, 2118.
- (59) Sun, S.; Ehrman, J.; Zhang, T.; Sun, Q.; Dyall, K. G.; Li, X. Scalar Breit Interaction for Molecular Calculations. *J. Chem. Phys.* **2023**, *158*, 171101.
- (60) Heß, B. A.; Marian, C. M.; Peyerimhoff, S. D. In *Modern Electronic Structure Theory*, Part I; Yarkony, D. R., Ed.; World Scientific, 1995; pp 152–278.
- (61) Dyall, K. G.; Fægri, Jr., K. Introduction to Relativistic Quantum Chemistry; Oxford University Press: New York, 2007.
- (62) Visscher, L.; Saue, T. Approximate relativistic electronic structure methods based on the quaternion modified Dirac equation. *J. Chem. Phys.* **2000**, *113*, 3996–4002.
- (63) Fleig, T.; Visscher, L. Large-scale electron correlation calculations in the framework of the spin-free dirac formalism: the Au2 molecule revisited. *Chem. Phys.* **2005**, *311*, 113–120.
- (64) Cheng, L.; Gauss, J. Analytical evaluation of first-order electrical properties based on the spin-free Dirac-Coulomb Hamiltonian. *J. Chem. Phys.* **2011**, *134*, 244112.

- (65) Cheng, L.; Stopkowicz, S.; Gauss, J. Spin-free Dirac-Coulomb calculations augmented with a perturbative treatment of spin-orbit effects at the Hartree-Fock level. J. Chem. Phys. 2013, 139, 214114.
- (66) Lipparini, F.; Gauss, J. Cost-Effective Treatment of Scalar Relativistic Effects for Multireference Systems: A CASSCF Implementation Based on the Spin-free Dirac-Coulomb Hamiltonian. J. Chem. Theory Comput. 2016, 12, 4284–4295.
- (67) Mann, J. B.; Johnson, W. R. Breit Interaction in Multielectron Atoms. *Phys. Rev. A* 1971, 4, 41–51.
- (68) Huang, K.-N.; Aoyagi, M.; Chen, M. H.; Crasemann, B.; Mark, H. Neutral-Atom Electron Binding Energies from Relaxed-Orbital Relativistic Hartree-Fock-Slater Calculations 2 ≤ Z ≤ 106. At. Data Nucl. Data Tables 1976, 18, 243–291.
- (69) Thierfelder, C.; Schwerdtfeger, P. Quantum Electrodynamic Corrections for the Valence Shell in Heavy Many-electron Atoms. *Phys. Rev. A* **2010**, *82*, 062503.
- (70) Chantler, C.; Nguyen, T.; Lowe, J.; Grant, I. Convergence of the Breit Interaction in Self-Consistent and Configuration-Interaction Approaches. *Phys. Rev. A* 2014, 90, 062504.
- (71) Pyykkö, P. The Physics behind Chemistry and the Periodic Table. *Chem. Rev.* **2012**, 112, 371–384.
- (72) Liu, W.; Lindgren, I. Going beyond "No-pair Relativistic Quantum Chemistry". *J. Chem. Phys.* **2013**, *139*, 014108.
- (73) Liu, W. Advances in Relativistic Molecular Quantum Mechanics. *Phys. Rep.* **2014**, *537*, 59–89.
- (74) Kozioł, K.; Giménez, C. A.; Aucar, G. A. Breit Corrections to Individual Atomic and Molecular Orbital Energies. J. Chem. Phys. 2018, 148, 044113.

- (75) Liu, W. Essentials of Relativistic Quantum Chemistry. J. Chem. Phys. **2020**, 152, 180901.
- (76) Sun, S.; Stetina, T. F.; Zhang, T.; Hu, H.; Valeev, E. F.; Sun, Q.; Li, X. Efficient Four-Component Dirac-Coulomb-Gaunt Hartree-Fock in the Pauli Spinor Representation.

 J. Chem. Theory Comput. 2021, 17, 3388-3402.
- (77) Sun, S.; Ehrman, J. N.; Sun, Q.; Li, X. Efficient Evaluation of the Breit Operator in the Pauli Spinor Basis. *J. Chem. Phys.* **2022**, *157*, 064112.
- (78) Williams-Young, D. B.; Petrone, A.; Sun, S.; Stetina, T. F.; Lestrange, P.; Hoyer, C. E.; Nascimento, D. R.; Koulias, L.; Wildman, A.; Kasper, J.; Goings, J. J.; Ding, F.; DePrince III, A. E.; Valeev, E. F.; Li, X. The Chronus Quantum (ChronusQ) Software Package. WIREs Comput. Mol. Sci. 2020, 10, e1436.
- (79) Roos, B. O.; Lindh, R.; Malmqvist, P.-A.; Veryazov, V.; Widmark, P.-O. Main Group Atoms and Dimers Studied with a New Relativistic ANO Basis Set. *J. Phys. Chem. A* **2004**, *108*, 2851–2858.
- (80) Pritchard, B. P.; Altarawy, D.; Didier, B.; Gibson, T. D.; Windus, T. L. New Basis Set Exchange: An Open, Up-to-Date Resource for the Molecular Sciences Community. **2019**, *59*, 4814–4820.
- (81) Kramida, A.; Ralchenko, Y.; Reader, J.; NIST ASD Team, NIST Atomic Spectra Database (version 5.6.1). https://physics.nist.gov/asd, 2018; National Institute of Standards and Technology, Gaithersburg, MD.

TOC Graphic

